Konversi 14(2) (2025) 55–62

KONVERSI
Homepage:
https://ppjp.ulm.ac.id/journal/index.php/konversi

Organic linker functionalization with chemical groups: A theoretical approach

Chinyere A. Anyama[1,*], Emmanuel A. Anyama[2], Ayi A. Ayi[1]

[1]*Department of Pure and Applied Chemistry, University of Calabar, Calabar 540221, Nigeria*

[2]*Department of Pharmacology, University of Calabar, Calabar 540221, Nigeria*

ARTICLE INFO

Article history:

Received: 06 September 2025
Received in revised form: 14 October 2025
Accepted: 20 October 2025

Keywords:

Ligands, functionalization, MOFs, energy gap, reactivity

ABSTRACT

Phenyl-2-pyridyl ketoxime (herein PPKO) with formula $C_{12}H_{10}N_2O$ and its CH_3, OH, NH_2, and NO_2 modified forms were optimized with Gaussian 09 using B3LYP (Beckes' 3-parameter exchange with Lee-Yang-Parr correlation energy) functional and 6-311+ G(d,p) basis set. Their structural, spectroscopic and molecular properties were investigated at same molecular level. The HOMO-LUMO energy was used to calculate the quantum descriptors to gain insight into their energy gap, reactivity and stability. From our result, we observed a narrowing of the energy gap of PPKO (0.184 eV) to 0.180 eV, 0.176 eV, 0.166 eV and 0.149 eV in CH_3-PPKO, OH - PPKO, NH2-PPKO and NO2-PPKO respectively. The optical performance was calculated with Time dependent Self Consistent Field (TD-SCF) and Integral equation formalism polarizable continuum model (IEF-PCM). From our result, the absorption wavelength of PPKO (283 nm) was extended to 284 nm, 307 nm and 356 nm in OH-PPKO, NH_2-PPKO and NO_2-PPKO respectively. This observed red shift in absorption wavelength is attributed to π-π* transitions. From the simulated FTIR, the O-H stretch was observed at 3600 cm^{-1}, 3603 cm^{-1}, 3605 cm^{-1}, 3609 cm^{-1} and 3585 cm^{-1} for PPKO, CH_3-PPKO, OH-PPKO, NH_2-PPKO and NO_2-PPKO respectively. The perturbation energy which gives insight into intra molecular and inter molecular interactions between donor and acceptor orbitals was calculated with respect to the second-order Fock matrix perturbation theory. NO_2-PPKO showed the greatest perturbation energy (250.92 k/cal/mol) from transitions between π*C1-N6 and π*C4-C5 (donor and acceptor orbitals respectively).

1. Introduction

Phenyl-2-pyridyl ketoxime belongs to the family of oximes which are chemical compounds with the general molecular formula RR'C=NCH where R is an organic group, and R' hydrogen or an organic group [1]. Phenyl-2-pyridyl ketoxime has a unique bonding capability and is able to form terminal, chelating and bridging bonds with most transition metals forming metal complexes with Cu^{2+}, Fe^{2+}, Mn^{2+}, Ni^{2+}, Ag^{2+}, Co^{2+} amongst others [2-11]. Chemists have also found interest in oximes as ligands because they are able to form mono-, di-, tri- and polynuclear copper complexes many of which are important magnetic and redox active materials [3]. Copper oximes possess biological active sites which enable them to bind covalently or non-covalently to Deoxyribonucleic acid (DNA) [5]. Since the discovery of MOFs by Omar Yaghi [12], there has been a lot of research going on in the area of metal-organic frameworks (MOFs) [13-18]. Scientists have found MOFs to be interesting materials because of their attractive properties which make them useful in many areas such as adsorption [19], catalysis [20], magnetism [21], storage [22], drug delivery [23], sensors [24] amongst others.

MOFs are formed from inorganic metal cations and organic linkers (ligands) which act as antennas through which MOFs could absorb light. The properties of MOFs are highly dependent on the properties of the organic linker which makes the choice of ligand very important. Different types of linker have been reported in the syntheses of MOFs especially the carboxylates [25-28], pyridine [29-31], oximes [32-34] and many others. Improving or modifying the properties of MOFs could be achieved in various ways which includes mixing of ligands [35] and functionalization of ligands [36]. Adjusting the properties of phenyl-2-pyridyl ketoxime in the synthesis of these metal complexes could be an efficient technique in adjusting the properties of the metal complexes. Hendon *et al* showed that the optical properties of Ti-MIL-125 MOF can be tailored by functionalizing the ligands that make it up [37], Gregory et al reported tuning the adsorption properties of UiO-66 via Ligand Functionalization [38]. Tun-ability of MOFs with organic linker is of obvious importance because it offers unlimited possibility to design functional or multifunctional organic linker as well as unique chemical properties of organic groups. The purpose of this work is to investigate theoretically the possibility of adjusting the structure, energy gap and reactivity of PPKO directed towards the design of linker molecules which could form part of new complexes and MOF materials with enhanced properties. In this work, we perform a systematic comprehensive analysis focusing on the geometric characteristics, electronic structure, molecular properties, spectroscopic, optical absorption and reactivity of phenyl-2-pyridyl ketoxime (PPKO) functionalized with CH_3, OH, NH_2,

* Corresponding author.
Email: chinyereanyama@gmail.com
http://dx.doi.org/10.20527/k.v14i2.2379

This open access article is distributed under a Creative Commons Attribution (CC-BY-SA) 4.0 license

and NO_2 functional groups.

2. Computational Details

The structure of phenyl-2-pyridyl ketoxime (herein PPKO) with formula C12H10N2O was modified with CH3, OH, NH2 and NO2. and their structures were optimized with Gaussian 09W [39]. The computational package calculations and geometry optimization process were carried out using a density functional theory (DFT) approach using the B3LYP hybrid functional which combines three Becke exchange parameters with Lee, Yang, and Parr correlations and the 6-311+G(d,p) basis set [40] functional with 6-311+G (d,p) basis set. The optical performance of the compounds in water, dimethylsulfoxide (DMSO) and chloroform was analyzed using the Time-Dependent Self-Consistent Field (TD-SCF) method and the Integral Equation Formalism–Polarized Continuum Model (IEF-PCM) which provides high predictive capability in studying vibrational circular dichroism and molecular behavior in solution. Natural bond orbital (NBO) version 3.1 was used to study inter-molecular and intra-molecular charge transfer (ICT), conjugative interactions and electron density delocalization.

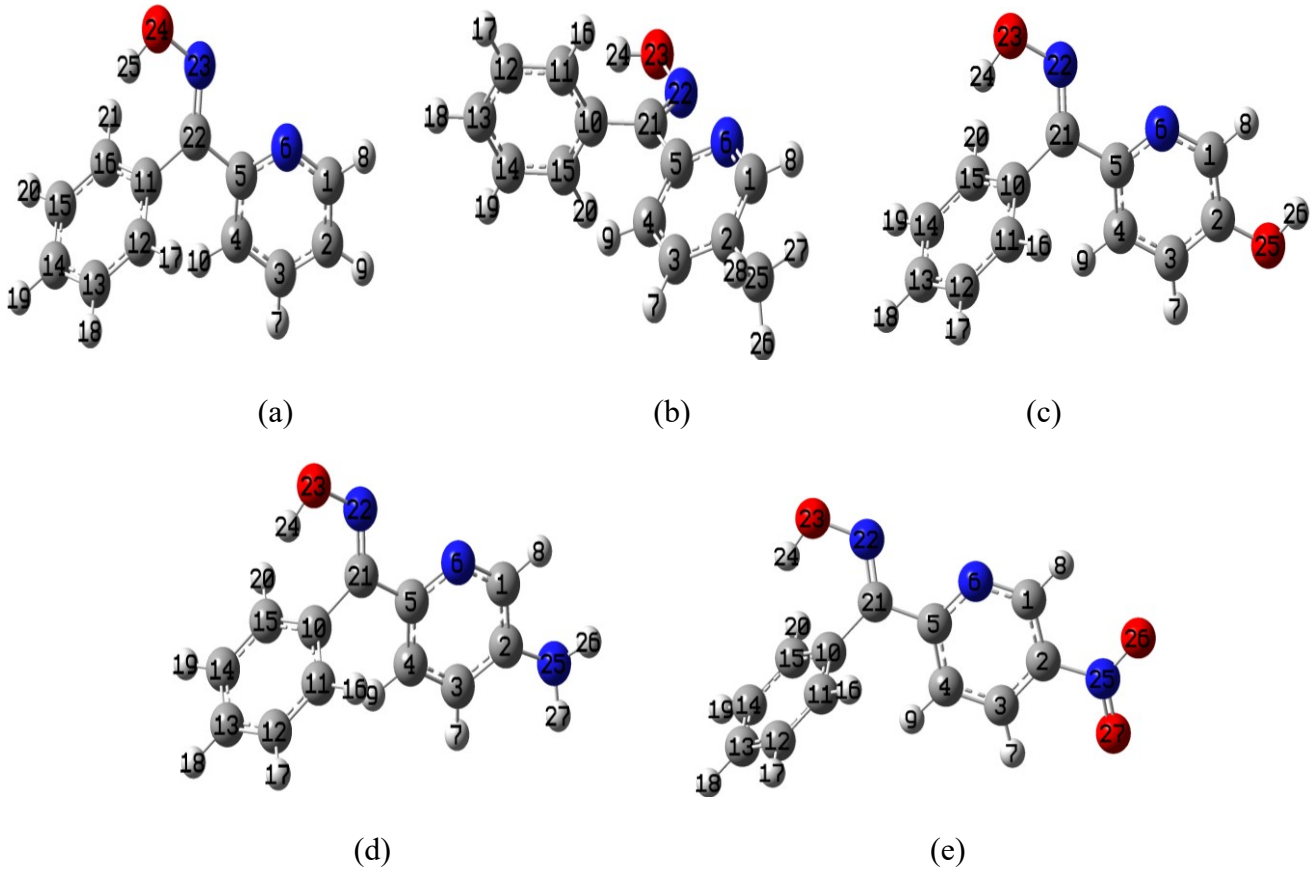

Fig. 1. Optimized structures of PPKO (a), CH3-PPKO (b), OH - PPKO (c), NH2-PPKO (d) and NO2-PPKO (e)

3. Results and Discussion

3.1. Geometrical parameters

The geometrical structure calculations include structure optimization, evaluation of bond lengths, bond angles, and dihedral angles with Gaussian 09 at the B3LYP 6-311 + G(d,p) level of theory; the overall results are shown in Figure 1 and Tables 1, 2 and 3. From the result obtained, changes in all three parameters were observed which could be attributed to the presence of the groups in the PPKO framework. C1-C2 which was 1.395Å for PPKO was observed as 1.400 Å, 1.399 Å, 1.409 Å and 1.396 Å in CH_3-PPKO, OH - PPKO, NH_2-PPKO and NO2-PPKO respectively. C2-C3 was 1.390 Å, 1.395 Å, 1.391 Å, 1.397 Å and 1.388 Å for PPKO, CH3-PPKO, OH - PPKO, NH2-PPKO and NO2-PPKO, respectively. C1-C2-C3 was observed as 117.9, 116.2, 118.1, 116.5 and 120.0 for PPKO, CH3-PPKO, OH - PPKO, NH2-PPKO and NO2-PPKO respectively. C1-N6-C5 was 118.1, 118.8, 118.7, 118.3 and 119.0 respectively for PPKO, CH_3-PPKO, OH - PPKO, NH_2-PPKO and NO_2-PPKO. C2-C3-C4 was 118.8, 119.8, 118.3, 119.2 and 117.5 for PPKO, CH_3-PPKO, OH - PPKO, NH_2-PPKO and NO_2-PPKO respectively. There were also changes in the dihedral angles, C5-C22-C11-C16 was -109.2, -108.5, -108.4, -106.9 and -106.0 in PPKO, CH_3-PPKO, OH - PPKO, NH_2-PPKO and NO_2-PPKO respectively. C4-C5-C22-N23 was -155.8, -157.2, -157.9, -161.0 and -161.7 respectively for PPKO, CH_3-PPKO, OH - PPKO, NH_2-PPKO and NO_2-PPKO.

Table 1. Selected bond length of studied compounds

BOND LENGTH	PPKO	CH3- PPKO	OH- IPPKO	NH2- PPKO	NO2- PPKO
C1-C2	1.395	1.400	1.399	1.409	1.396
C1-N6	1.331	1.330	1.325	1.322	1.326
C2-C3	1.390	1.395	1.391	1.397	1.388
C3-C4	1.390	1.389	1.388	1.388	1.386
C4-C5	1.402	1.402	1.403	1.401	1.405
C5-N6	1.341	1.339	1.340	1.343	1.344

Table 2. Selected bond angles of studied compound

BOND ANGELS	PPKO	CH3- PPKO	OH- PPKO	NH2- PPKO	NO2- PPKO
C1-C2-C3	117.9	116.2	118.1	116.5	120.0
C1-N6-C5	118.1	118.3	118.8	119.0	118.7
C2-C3-C4	118.8	119.8	118.3	119.2	117.5
C3-C4-C5	119.0	119.1	119.7	119.8	119.2
C4-C5-N6	122.1	121.6	121.3	120.9	122.1
N6-C5-C22	117.8	118.1	118.2	118.3	117.8

Table 3. Selected dihedral angles of studied compounds

DIHEDRAL ANGLES	PPKO	CH3-PPKO	OH-lPPKO	NH2-PPKO	NO2-PPKO
C1-N6-C5-C22	-178.5	-178.5	-178.3	-178.6	-178.9
C3-C4-C5-C22	178.6	178.5	178.4	178.6	179.0
C4-C5-C22-N23	-155.8	-157.2	-157.9	-161.0	-161.7
C5-C22-C11-C16	-109.2	-108.5	-108.4	-106.9	-106.0
C11-C22-C5-N6	-156.6	-158.0	-158.9	-161.8	-162.5

3.2. Frontier molecular orbitals (FMOs)

HOMO as the highest occupied molecular orbital and LUMO as the lowest unoccupied orbital (LUMO) are known as frontier molecular orbitals (FMO). The energy distance between them is used to describe the level of chemical reactivity and kinetic stability of a molecule [41]. A molecule with a small energy gap termed a soft molecule is generally associated with a high chemical reactivity and low kinetic stability [42]. The HOMO and LUMO structures and the orbitals for the studied molecules are shown in Figure 2. From our result the HOMO and LUMO of PPKO are the 52^{th} and 53^{th} orbital, the HOMO and LUMO of CH_3-PPKO, OH - PPKO and NH_2-PPKO are the 56^{th} and 57^{th} orbital, the HOMO and LUMO of NO_2-PPKO are the 63^{th} and 64^{th} orbital. The HOMO of PPKO is located over the C1-C2 and C4-C5-N6 bonds of the pyridyl ring and C=N and O atom of the ketoxime while the LUMO is delocalized over C2, C4, C5-C22 bond and N- atom of the pyridyl ring, the phenyl carbon atoms and the N- atom of the ketoxime. The HOMO of CH_3-PPKO is located over C1-C2 bond, C4-C5-N6 bond, CH3 group, C=N and O atom while LUMO is located over C2, C3, C5, N6, C5-C22 bond, N atom of ketoxime and the phenyl carbon atoms. The HOMO of OH - PPKO is located over C1-C2-C3 and C4-C5-N6 bond of the pyridyl ring, C=N, O atom of ketoxime and OH group while the LUMO is localized over C1-C2 and C5-C22 bonds, C3, N6, phenyl carbon atoms and N- atom of ketoxime. The HOMO of NH_2-PPKO is located over C1-C2-C3 and C4-C5-N6 bonds, NH_2 group, C=N and O atom of the ketoxime while the LUMO is located over C1-C2 and C5-C22, N- atom of the ketoxime and phenyl carbon atoms. The HOMO of NO_2-PPKO is located over C1-C2 and C4-C5-N6 bonds, C=N, O atom of ketoxime, C10-C15 and C13-C14 bonds of the phenyl ring while LUMO is located over the NO_2 group, C1, C2, C3, C5 and N6 of the pyridyl group and the N atom of the ketoxime. These (HOMO→LUMO) transitions suggest that electron density transfer was generally from the pyridyl ring to the phenyl ring. It also suggests that CH_3, OH and NH_2 are electron rich while NO_2 is electron deficient. From these HOMO-LIMO transitions, we also observe that the ketoxime O atom is highly electron rich and so suggests that it could serve as coordination sites for highly electron deficient metal cations in MOF Frameworks.

3.3. Quantum chemical descriptors

The quantum chemical descriptors calculated with the famous Koopmans approximation [43] are presented in Table 4. On the basis of Koopmans approximation, the Ionization Potential (IP) and Electron Affinity (EA) are approximately equal to negative HOMO (- HOMO) and negative LUMO (- LUMO) respectively.

$$IP=-E_{HOMO} \quad (1)$$

$$EA=-E_{LUMO} \quad (2)$$

Using equations (3) – (7) the global reactivity descriptors were calculated as is reported in literature [16,25].

The hardness of the molecule is $\eta=(IP-EA)/2$. (3)

The chemical potential of the molecule is μ=-*(IP+EA)/2.* (4)

The softness(σ) of the molecule= 1/2η. (5)

The electronegativity of the molecule is χ = *(IP+EA)/2.* (6)

The electrophilicity index of the molecule is $\omega = \mu/2\eta 2$. (7)

From our result, NH2-PPKO with the lowest ionization potential value (0.217 eV) is the best donor while NO_2-PPKO with the highest electron affinity value of 0.119 eV is the best acceptor. We can also deduce from our result that the energy gap of PPKO (0.184 eV) was narrowed down to 0.180 eV, 0.176 eV, 0.166 eV and 0.149 eV in CH_3-PPKO, OH - PPKO, NH_2-PPKO and NO_2-PPKO respectively which is in good agreement with the softness values of 5.425, 5.528, 5.761, 6.023 and 6.673 for PPKO, CH_3-PPKO, OH - PPKO, NH_2-PPKO and NO_2-PPKO respectively. The lower the energy gap, the more reactive a molecule and so NO_2-PPKO with the lowest energy gap (0.149 eV) is the most reactive with the highest softness value of 6.673 which suggests it is less stable and most polarizable. These results show that functionalization of PPKO with these chemical groups narrowed the band gap of PPKO thereby increasing its reactivity. These properties which can be transferred from the linker (PPKO, CH_3-PPKO, OH - PPKO, NH_2-PPKO, NO_2-PPKO) to the metal complexes and MOFs during syntheses could enhance or modify their catalytic, semiconductor, reactivity and optoelectronic properties.

Table 4. Quantum chemical descriptors of studied compounds

	PPKO	CH_3-PPKO	OH - PPKO	NH_2-PPKO	NO_2-PPKO
E_{HOMO} (eV)	- 0.2467	-0.2402	-0.2341	- 0.2170	- 0.2697
E_{LUMO} (eV)	-0.0624	-0.0593	-0.0578	-0.0510	- 0.1199
ΔE_{gap} (eV)	0.1843	0.1808	0.1763	0.1660	0.1498
IP (eV)	0.2467	0.2402	0.2341	0.2170	0.2697
EA (eV)	0.0624	0.0593	0.0578	0.0510	0.1199
μ (eV)	-0.1545	-0.1498	-0.1460	-0.1346	-0.1948
χ (eV)	0.1545	0.1240	0.1460	0.1346	0.1948
η (eV)	0.0921	0.0904	0.0881	0.0830	0.0749
σ (eV)	5.4256	5.5282	5.6711	6.0233	6.6737
ω (ev)	0.1296	0.1214	0.1208	0.1092	0.2534

3.4. Vibrational analysis

Vibrational analysis enables us to reveal vibrational modes that reflect the characteristic structure of the molecule being analyzed. For a non-linear molecule containing N atoms, theory suggests that there are up to (3N–6) fundamental vibrational modes that can be observed [44]. Hence, PPKO molecule has 25 atoms with 69 vibrations, CH_3--PPKO has 28 atoms with 69 vibrations, OH - PPKO has 26 atoms with 72 vibrations, NH_2-PPKO and NO_2-PPKO have 27 atoms each with 75 vibrations. The IR spectra of the studied molecules are presented in Figure 2 while the frequencies, intensities and vibrational assignments are presented in S9. C-C vibration was observed at 1288 cm^{-1}, 1284 cm^{-1}, 1281 cm^{-1}, 1288 cm^{-1} and 1302 cm^{-1} for PPKO, CH_3-PPKO, OH-PPKO, NH_2-PPKO and NO_2-PPKO respectively. C=C stretching vibrations was observed at 1596 cm^{-1}, 1588 cm^{-1} and 1508 cm^{-1}, 1596 cm^{-1} and 1625 cm^{-1} for PPKO, CH_3-PPKO, OH-PKO, NH_2-PPKO and NO_2-PPKO respectively. C=N vibrations was observed at 1619 cm^{-1}, 1642 cm^{-1}, 1616 cm^{-1} and 1595 cm^{-1} for CH_3-PPKO, OH-PKO, NH_2-PPKO and NO_2-PPKO respectively. C-H stretching vibrations for PPKO was observed at 3145 cm^{-1} while for CH_3-PPKO, OH-PPKO, NH_2-PPKO and NO_2-PPKO it was observed at 3130 cm^{-1}, 3106 cm^{-1} 3115 cm^{-1} and 3194 cm^{-1} respectively while the O-H stretch is observed at 3600 cm^{-1}, 3603 cm^{-1}, 3605 cm^{-1}, 3609 cm^{-1} and 3585 cm^{-1} for PPKO, CH_3-PPKO, OH-PPKO, NH_2-PPKO and NO_2-PPKO respectively. NH_2 symmetric, asymmetric and bending vibrations were observed at 3573 cm^{-1}, 3673 cm^{-1} and 1662 cm^{-1}respectively for NH_2-PPKO while the CH_3 vibrations for CH_3-PPKO was observed at 3024 cm^{-1}. Stronger bonds absorb at higher frequencies due to their greater bond force constants resulting in higher energy vibrations (45). From our results, the bonds formed between PPKO and the functional groups are very strong bonds which are very essential for overall framework stability of MOFs.

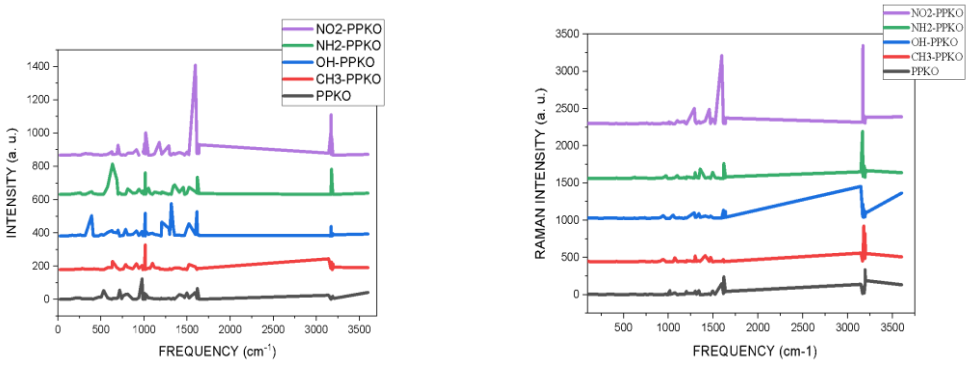

(a) (b)

Fig. 2. Simulated IR (a) and Raman (b) spectra of studied compounds

3.5. Spectroscopic analysis of UV-Vis

The electronic behavior of the molecules were estimated by TD-SCF/IEF-PCM/B3LYP 6-311 + G (d,p). The UV-visible spectra of the molecules in water, dimethyl sulfoxide and chloroform are presented in Figure 3 while the wave lengths (λ_{max}), excitation energy (E) and oscillator strengths are presented in S7, S8 and S9. From our result, the spectra of the studied compounds show one peak each at wavelengths 283 nm for PPKO and CH_3-PPKO, 284 nm, 307 nm and 356 nm (λ_{max}) for OH-PPKO, NH_2-PPKO and NO_2-PPKO in water, In DMSO 283 nm was observed for PPKO and CH_3-PPKO, 285 nm, 308 nm and 356 nm for OH-PPKO, NH_2-PPKO and NO_2-PPKO while 286 nm for PPKO and CH_3-PPKO, 285 nm, 307 nm and 356 nm were observed for OH-PPKO, NH_2-PPKO and NO_2-PPKO respectively in chloroform. These transitions corresponding to $\pi \rightarrow \pi^*$ transition is governed by HOMO→LUMO excitation. From our result, we observe that absorption wavelength of PPKO was extended towards the visible region in the functionalized forms. Red Shift typically suggests, weaker bonding or lower HOMO–LUMO gap, a more delocalized electronic system, lower stability and more reactivity [46]. This is in good agreement with other results from quantum chemical descriptors. One of the major flaws of PPKO as an organic linker is its poor extension in the visible region. With the introduction of these functional groups, this flaw is corrected. This will be passed onto the MOFs during syntheses thereby increasing their optical performance.

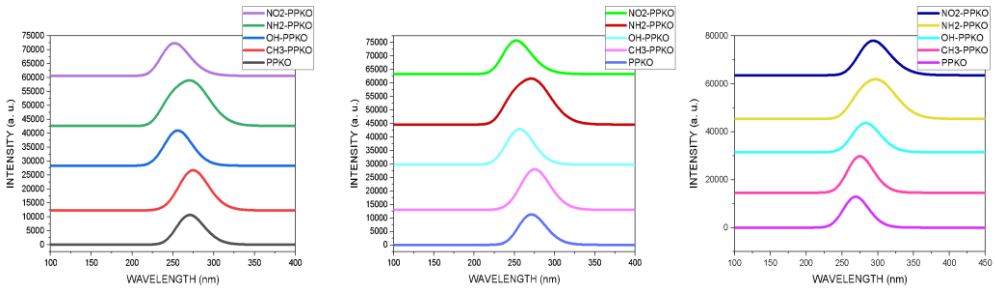

(a) (b) (c)

Fig. 3. UV spectral simulations for the selected compounds in water (a), DMSO (b), and chloroform (c) calculated with B3LYP/6-311 +G (d,p) basis sets

3.6. Analysis of natural bonding orbital (NBO)

Natural bond orbital (NBO) analysis provides an effective method for analyzing intra- and inter molecular bonding interactions between bonds and also presents a suitable basis for investigating charge transfer or conjugative interactions in molecules [47]. The greater the perturbation energy value, the stronger the interaction between the electron donors and the more the conjugation of the system [48-49]. The second-order perturbation energy values of PPKO, CH_3-PPKO, OH - PKO, NH_2-PPKO and NO_2-PPKO were assessed with regard to the second-order Fock matrix perturbation theory using DFT/B3LYP/6-311+G (d, p) functional. The most interacting NBOs are presented in S1, S2, S3, and S4 for PPKO, CH_3-PPKO, OH-PKO, NH_2-PPKO and NO_2-PPKO respectively. From our result, molecular interactions in the studied molecules is observed by a π-π*, π*-π* transition between C–C orbitals and π-LP, π-LP*, LP-π*, LP-LP*, LP*-π* transition between C-C, O-C, N-C and O-N orbitals. Intramolecular hyperconjugative effects in the system are generated through the interaction and overlapping of orbitals between π*C1-N6 and π*C4-C5 for PPKO, LP(1)C2 and π*C1-N6 for CH_3-PPKO, π*C1-N6 and π*C4-C5 for OH-PPKO, LP(1)C5 and π*C1-C6 for NH_2-PPKO, π*C5-N6 and π*C3-C4 for NO_2-PPKO producing stabilization energies 250.92 K/cal/mol, 89.04 K/cal/mol, 170.08 K/cal/mol, 75.72K/cal/mol and 228 K/cal/mol for PPKO, CH_3-PPKO, OH - PKO, NH_2-PPKO and NO_2-PPKO respectively. Systems requiring greater perturbation energy tend to be more stable due to their high conjugation. Increased conjugation decreases the reactivity of the molecule. From our result, PPKO has highest perturbation energy which suggests that it is more stable and less reactive which agrees with the fact that it had the highest energy (ΔEgap). This clearly shows that the functional groups made PPKO more reactive, a potential for application in MOF syntheses.

3.7. Charge analysis

Mulliken charges are the results of Mulliken population analysis (MPA) to determine partial atomic charges based on computational chemistry calculations with a linear combination approach of atomic orbitals [58]. MPA analysis is highly effective in determining the size, structure and electronic distribution of the HOMO-LUMO orbitals, which is key in predicting the concentration of electrons in the studied molecules. A plot of Mulliken charge distribution with the number of atoms for the molecules is presented in Figure 4. From our result, the most electropositive atom (most susceptible to nucleophillic attack) in PPKO is C11 (1.588 a. u.) while the most electronegative atom (most susceptible to electrophillic attack is C22 (-0.959 a. u.). The most electropositive atom (most susceptible to nucleophillic attack) in CH_3-PPKO is C10 (1.261a. u.) while the most electronegative atom (most susceptible to electrophillic attack) is C5 (-0.870 a. u.). The most electropositive atom (most susceptible to nucleophillic attack) in OH-PPKO is C10 (0.929 a. u.) while the most electronegative atom (most susceptible to electrophillic attack is C5 (-0.780 a. u.). The most electropositive atom (most susceptible to nucleophillic attack) in NH_2-PPKO is C10 (1.160 a. u.) while the most electronegative atom (most susceptible to electrophillic attack) is C5 (-0.760 a. u.). The most electropositive atom (most susceptible to nucleophillic attack) in NO_2-PPKO is C10 (1.400

a. u.) and the most electronegative atom (most susceptible to electrophillic attack) is C5 (-0.602 a. u.). Our result suggests more interaction within the pyridyl ring (C5 and C10) in the functionalized PPKO molecules which is attributed to the presence of the chemical groups. Also from our result, C2 (point of attachment of chemical groups) atomic charge was positive for PPKO and CH_3-PPKO (0.062 a. u. and 0.784 a. u. respectively) while for OH - PPKO, NH_2-PPKO and NO_2-PPKO it was negative (-0.128 a. u., -0.025 a. u. and -0.068 a. u. respectively). This also suggests changes in electron density caused by the presence of the chemical groups on the C2 atom. These electron movements are necessary for reactivity in both PPKO as an organic linker in MOF syntheses and also for the overall reactivity of MOF frameworks.

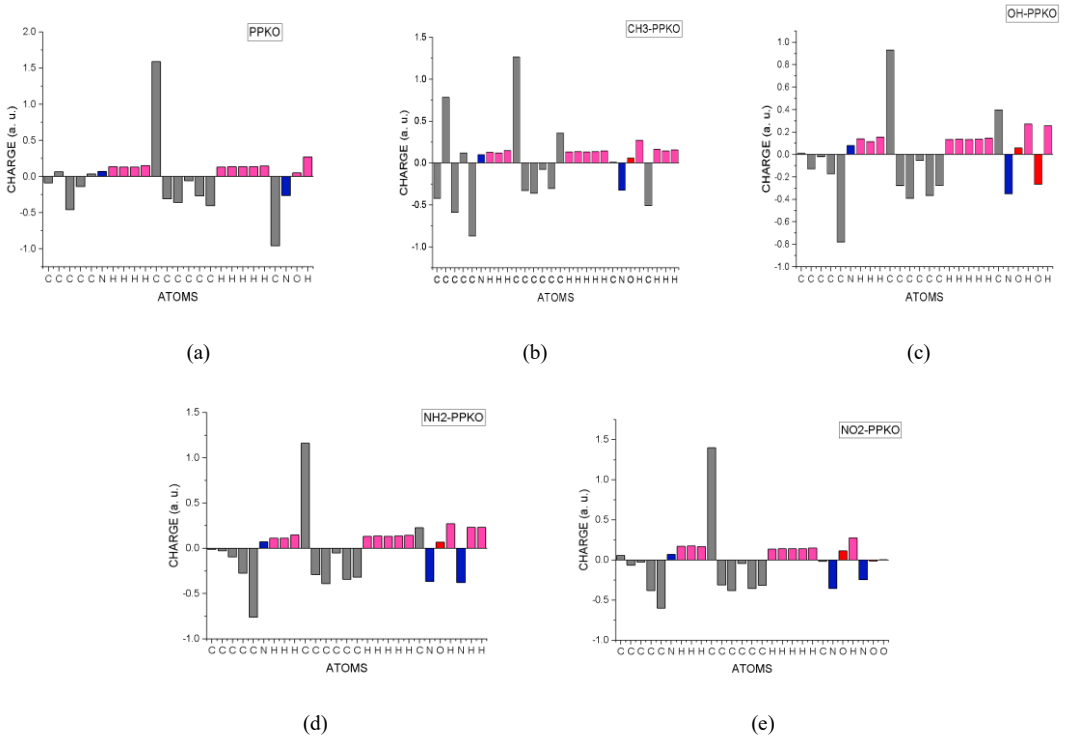

Fig. 4. A graphical distribution of Mulliken atomic charges along the molecular atoms for PPKO (a), CH_3-PPKO (b), OH - PPKO (c) and NH_2-BTC (d) and NO_2-PPKO respectively

4. Conclusion

This research was carried out to adjust the structure, energy gap, spectroscopic properties and reactivity of phenyl 2-pyridyl ketoxime. From the result obtained changes in all three geometrical parameters were observed which can be attributed to the presence of the groups in the PPKO framework. For instance, C1-C2 which was 1.395Å for PPKO was observed as 1.400 Å, 1.399 Å, 1.409 Å and 1.396 Å in CH_3-PPKO, OH-PPKO, NH_2-PPKO and NO_2-PPKO respectively. From our HOMO-LUMO energy calculation results, the energy gap of PPKO (0.184 eV) was narrowed down in all the functionalized forms which shows that the reactivity of PPKO was increased. The lower the energy gap, the more reactive a molecule and so NO_2-PPKO with the lowest energy gap (0.149 eV) was the most reactive with the highest softness value of 6.673. From our FTIR results, the bonds formed between PPKO and the functional groups are very strong bonds which are highly essential for overall framework stability of MOFs. From our UV results, we observed that absorption wavelength of PPKO was extended towards the visible region in the functionalized forms. Red Shift typically suggests, weaker bonding or lower HOMO–LUMO gap, a more delocalized electronic system, lower stability and more reactivity. These properties which could be transferred from the linker (PPKO, CH_3-PPKO, OH-PPKO, NH_2-PPKO, NO_2-PPKO) to the metal complexes and MOFs during syntheses could enhance or modify their energy gap, reactivity, optoelectronic, catalytic and semi-conductor properties thereby giving a wide array of unique hybrid materials that could be useful in relevant areas.

Conflict of interest

The authors declare no conflict of interest.

Acknowledgments

We acknowledge the University of Calabar for providing enabling academic environment.

References

[1] A. A. I. Abd-Elmageed, S. M. Ibrahim and A. F. Al-Hossainy, Synthesis, DFT studies, fabrication, and optical characterization of the (Zn CMC)TF polymer (organic/inorganic) as an optoelectronic device, *New J. Chem.* 44 (2020) 8621–8637.

[2] M. A. Afzai and S. H. Naqib, A DFT based first-principles investigation of optoelectronic and structural properties of Bi_2Te_2Se, *Phys. Scr.* 96 (2021) 045810.

[3] M. D. Allendorf, R. J. T. Houk, L. Andruszkiewicz, A. A. Talin, J. Pikarsky et al., Stress-induced chemical detection using flexible metal–organic frameworks, *J. Am. Chem. Soc.* 130 (2008) 14404–14405.

[4] J. An, S. J. Geib and N. L. Rosi, High and selective CO_2 uptake in a

cobalt adeninate metal-organic framework exhibiting pyridine and amino-decorated pores, *J. Am. Chem. Soc.* 132 (2010) 38–39.

[5] C. A. Anyama, B. I. Ita, A. A. Ayi, H. Loius, E. D. D. Okon et al., Experimental and density functional theory studies on a zinc(II) coordination polymer constructed with 1,3,5-benzenetricarboxylic acid and derived nanocomposites from activated carbon, *ACS Omega* 6 (2021) 28967–28982.

[6] N. S. Babu and A. H. Vuia, Theoretical studies of optoelectronic and photovoltaic properties of D–A polymer monomers by density functional theory (DFT), *Des. Monomers Polym.* 24 (2021) 226–239.

[7] C. A. Bauer, T. V. Timofeeva, T. B. Settersten, B. D. Patterson, V. H. Liu et al., Influence of connectivity and porosity on ligand-based luminescence in zinc metal–organic frameworks, *J. Am. Chem. Soc.* 129 (2007) 7136–7144.

[8] M. Beatrice, S. Fabrice, B. Sandrine, P. L. L., D. Thomas et al., Effect of the ligand functionalization on the acid–base properties of flexible MOFs, *Microporous Mesoporous Mater.* 195 (2014) 197–204.

[9] M. Carcelli, P. Cozzini, R. Marroni, P. Pelagatti, C. Pelizzi and P. Sgarabotto, Unusual coordination mode of a 2-pyridyl ketone oxime ligand in bis(4-butylphenyl 2-pyridyl ketone oximate)palladium(II), *Inorg. Chim. Acta* 285 (1999) 138–141.

[10] C. G. Carson, A. J. Brown, D. S. Sholl and S. Nair, Sonochemical synthesis and characterization of submicrometer crystals of the metal-organic framework Cu[(hfipbb)(H_2hfipbb)$_{0.5}$], *Cryst. Growth Des.* 11 (2011) 4505–4510.

[11] B. D. Chandler, D. T. Cramb and G. K. H. Shimizu, Microporous metal–organic frameworks formed in a stepwise manner from luminescent building blocks, *J. Am. Chem. Soc.* 128 (2006) 10403–10412.

[12] B. L. Chen, L. B. Wang, Y. Q. Xiao, F. R. Fronczek, M. Xue et al., A luminescent metal-organic framework with Lewis basic pyridyl sites for sensing of metal ions, *Angew. Chem. Int. Ed.* 48 (2009) 500–503.

[13] J. Chen, H. Zhao, A. Farajtabar, P. Zhu, A. Jouyban et al., Equilibrium solubility of amrinone in aqueous co-solvent solutions reconsidered: Quantitative molecular surface, inter/intra-molecular interactions and solvation thermodynamics analysis, *J. Mol. Liq.* 355 (2022) 118995.

[14] W. Q. Chen, Y. M. Chen, T. Lei, W. Liu and Y. Li, V-shaped Fe(III) and linear Fe(II)/Fe(III)/Fe(II) complexes supported by phenyl-pyridine-2-yl-methanone oxime ligand: Solvothermal syntheses, structures and magnetic property, *Inorg. Chem. Commun.* 19 (2012) 4–9.

[15] A. A. Chinyere, B. A. Providence, E. I. Bassey, J. M. Idongesit and A. A. Ayi, Metal-organic frameworks as precursor for metal oxide nanostructures part I: MOF-derived copper oxide embedded in carbon matrix, *Adv. J. Chem. Sect. A* 2 (2019) 234–244.

[16] C. H. Hendon, D. Tiana, C. Fontecave, L. Sanchez et al., Engineering the optical response of the titanium-MIL-125 metal-organic framework through ligand functionalization, *J. Am. Chem. Soc.* 135 (2013) 10942–10945.

[17] C. G. E., I. M., S. D. G., A. T., V. N. et al., Synthesis and characterisation of new Ni_2Mn, Ni_2Mn_2 and Mn_8 clusters by the use of 2-pyridyl oximes, *Polyhedron* 171 (2019) 330–337.

[18] C. J. M., P. A. W., S. P., F. A. Dolos, C. L., G. C., S. P. P. and E. K. B., The use of methylsalicyloxime in manganese chemistry: A [Mn^3III] triangle and its oxidation to a [Mn^4IVCe$_2$III] rod, *Inorg. Chim. Acta* 360 (2007) 3932–3940.

[19] Y. Cui, H. Xu, Y. Yue, Z. Guo, J. Yu et al., A luminescent mixed-lanthanide metal–organic framework thermometer, *J. Am. Chem. Soc.* 134 (2012) 3979–3982.

[20] R. Dennington, T. A. Keith and J. M. Millam, *GaussView 6.0*, Semichem Inc., Shawnee Mission, KS, USA, 2016.

[21] C. Dey, T. Kundu, B. P. Biswal, A. Mallick and R. Banerjee, Crystalline metal-organic frameworks (MOFs): Synthesis, structure and function, *Acta Crystallogr. B* 70 (2014) 3–10.

[22] E. E., H. M. Louis, A. A. Chinyere, O. O. Joseph, M. U. Patrick et al., Experimental and density functional theory studies on adsorption behavior of selected gas molecules on Mg(II) coordination polymer constructed with 1,3,5-benzenetricarboxylates, *J. Mol. Struct.* 1220 (2020) 128641.

[23] D. D. Gemechis, P. Ravindr, G. Chansi and B. Lalit, Tailoring the electronic property of Zn-BTC metal–organic framework via ligand functionalization: An ab initio investigation, *RSC Adv.* 9 (2019) 13959–14579.

[24] E. C. Gregory, K. Min, M. C. Seth and S. W. Krista, Tuning the adsorption properties of UiO-66 via ligand functionalization, *Langmuir* 28 (2012) 15606–15613.

[25] M. Hołyńska, Iridium(III) products isolated in a reaction of $IrCl_3$ with phenyl-2-pyridyl ketoxime, *Z. Kristallogr. – Cryst. Mater.* 228 (2013) 72–76.

[26] M. Hołyńska, Structural variety and magnetic properties of oxime-bridged copper(II) complexes, *J. Mol. Struct.* 1098 (2015) 175–180.

[27] M. J. Frisch, G. W. Trucks, H. B. Schlegel, G. E. Scuseria, M. A. Robb, J. R. et al., *Gaussian 09, Revision C.02*, Gaussian, Inc., Wallingford, CT, 2009.

[28] M. Javier, A. Iolinda, B. Anna, C. Alessandra and G. Mauro, Tetranuclear zinc complexes of ligands containing the 2-pyridyl oxime chelating site, *Inorg. Chim. Acta* 361 (2008) 2677–2682.

[29] F. Ke, L. Wang and J. Zhu, Facile fabrication of CdS–metal-organic framework nanocomposites with enhanced visible-light photocatalytic activity for organic transformation, *Nano Res.* 8 (2015) 1834–1846.

[30] S. Keke, L. Ling, Y. XiaoLan, L. Li, M. Qingtao et al., Functionalization of mixed-ligand metal-organic frameworks as transport vehicles for drugs, *J. Colloid Interface Sci.* 486 (2017) 128–135.

[31] H. C. Khera, S. G. Mittal, M. Mohan and A. K. Srivasta, Transition metal chemistry of oxime containing ligands: Part III—Complexes of Fe(II), Co(II) and Ni(II) with pyridine-2-aldoxime and 6-methylpyridine-2-aldoxime, (1977).

[32] K. Konstas, T. Osl, Y. Yang, M. Batten, N. Burke et al., Methane storage in metal-organic frameworks, *J. Mater. Chem.* 22 (2012) 16698–16708.

[33] T. Koopmans, About the assignment of wave functions and eigenvalues to the individual electrons of an atom, *Phys. Polonica* (1993) 104–113.

[34] C. A. C. Kramer, A. R. L. da Silva, P. de Lima-Neto and L. S. de Carvalho, Computational approach in lignin structural models: Influence of non-covalent intramolecular interactions on β-O-4 bond properties, *J. Mol. Struct.* 1251 (2022) 131938.

[35] M. Kurmoo, Magnetic metal–organic frameworks, *Chem. Soc. Rev.* 38 (2009) 1353–1379.

[36] H. Li, M. Eddaoudi, M. O'Keeffe and O. M. Yaghi, Design and synthesis of an exceptionally stable and highly porous metal-organic framework, *Nature* 402 (1999) 276–279.

[37] J. R. Li, R. J. Kuppler and H.-C. Zhou, Selective gas adsorption and separation in metal-organic frameworks, *Chem. Soc. Rev.* 38 (2009) 1477–1504.

[38] R. Li, J. Lu, D. Li, S. Cheng and J. Dou, Syntheses, structures, in vitro cytotoxicities and DNA-binding properties of four copper complexes based on a phenyl 2-pyridyl ketoxime ligand, *Transition Met. Chem.* 39 (2014) 507–517.

[39] X. Lin, I. Telepeni, A. J. Blake, A. Dailly, C. M. Brown et al., High capacity hydrogen adsorption in Cu(II) tetracarboxylate framework materials: Role of pore size, ligand functionalization and exposed metal sites, *J. Am. Chem. Soc.* 131 (2009) 2159–2171.

[40] Z. Z. Lu, R. Zhang, Y. Z. Li, Z. J. Guo and H. G. Zheng, Solvatochromic behaviour of a nanotubular metal-organic framework for sensing small molecules, *J. Am. Chem. Soc.* 133 (2011) 4172–4174.

[41] C. J. Milios, T. C. Stamatatos, P. Kyritsis, A. Terzis, C. P. Raptopoulou et al., Phenyl 2-pyridyl ketone and its oxime in manganese carboxylate chemistry: Synthesis, characterisation, X-ray studies and magnetic properties of mononuclear, trinuclear and octanuclear complexes, *Eur. J. Inorg. Chem.* 2004 (2004) 2885–2901.

[42] Y. Morikawa, K. Manseki and S. Yanagida, Intermolecular interaction as origin of red shifts in absorption spectra of zinc-phthalocyanine from first-principles, *J. Phys. Chem. A* 117 (2013) 11246–11253.

[43] R. S. Mulliken, Electronic population analysis on LCAO-MO molecular wave functions, *J. Chem. Phys.* 23 (1955) 1833–1840.

[44] N. S. Nurettin, D. Sahin and Y. Mustafa, Preparation and characterization of bi-metallic and tri-metallic metal organic frameworks based on trimesic acid and Co(II), Ni(II) and Cu(II) ions, *J. Electron. Mater.* 46 (2017) 790–801.

[45] H. Ohi, Y. Tachi and S. Itoh, Supramolecular and coordination polymer complexes supported by a tripodal tripyridine ligand containing a 1,3,5-triethylbenzene spacer, *Inorg. Chem.* 43 (2004) 4561–4563.

[46] A. A. Olajuyigbe, A. A. Khalil and C. George, Mn_3 single-molecule magnets and Mn_6/Mn_9 clusters from the use of methyl 2-pyridyl ketone oxime in manganese phosphinate and phosphonate chemistry, *Inorg. Chem.* 56 (2017) 11352–11364.

[47] R. G. Parr and W. Yang, Density functional approach to the frontier-electron theory of chemical reactivity, *J. Am. Chem. Soc.* 106 (1984) 4049–4050.

[48] R. G. Pearson, Principle of maximum hardness, *Acc. Chem. Res.* 26 (1993) 250–255.

[49] N. P. G. Roeges, *A Guide to the Complete Interpretation of Infrared Spectra of Organic Structures*, Wiley, New York, 1994.

[50] R. Szczęsny, E. Szłyk, A. Kozakiewicz and L. Dobrzańska, Thermal and structural characterization of copper(II) complexes with phenyl-2-pyridylketoxime (HPPK), *J. Therm. Anal. Calorim.* 128 (2017) 1591–1599.

[51] W. Z. Wang, H. Junli, Z. Qi, W. Lei, L. Ding, Y. Weimin and W. Wenjie, DFT exploration of metal ion–ligand binding: Toward rational design of chelating agent in semiconductor manufacturing, *Molecules* 29 (2024) 308.

[52] J. S. Y. Wong and W. T. Wong, Synthesis, structural characterization and reactivity of triosmium carbonyl clusters containing oxime ligands, *New J. Chem.* 26 (2002) 94–104.

[53] W. Xiang, Y. Zhang, H. Lin and C. J. Liu, Nanoparticle/metal-organic framework composites for catalytic applications: Current status and perspective, *Molecules* 22 (2017) 2103.

[54] S. Yanagisawa, T. Yasuda, K. Inagaki, Y. Morikawa, K. Manseki and S. Yanagida, Intermolecular interaction as origin of red shifts in absorption spectra of zinc-phthalocyanine from first-principles, *J. Phys. Chem. A* 117 (2013) 11246–11253.

[55] J. Z. Yin and G. X. Liu, Dichloridobis(phenyl 2-pyridyl ketone oxime)nickel(II) acetone solvate, *Acta Crystallogr. E* 65 (2009) m155.

[56] W. Zhang, Z. Chen, M. Al-Naji, P. Guo, S. Cwik et al., Simultaneous introduction of various palladium active sites into MOF via one-pot synthesis: Pd@$[Cu_{3-x}Pd_x(BTC)_2]_n$, *Dalton Trans.* 45 (2016) 14883–14887.

[57] I. Zubair, R. Ahmad, K. Sahar, J. Akram, Y. A. El-Badry et al., Tuning the optoelectronic properties of indacenodithiophene-based derivatives for efficient photovoltaic applications: A DFT approach, *Chem. Phys. Lett.* 793 (2022) 139459.

[58] W. Zhang, Z. Chen, M. Al-Naji, P. Guo, S. Cwik, et al., Simultaneous introduction of various palladium active sites into MOF via one-pot synthesis: Pd@[Cu3xPdx(BTC)2]n. *Dalton Transactions*, 45 (2016) 14883–14887.

[59] I. Zubair, R. Ahmad, K. Sahar, J. Akram, Y. A. El-Badry., et al. Tuning The Optoelectronc Properties of indacenodithiophene Based Derivatives for Efficient Photovoltaic Applications: A DFT approach. *Chemical Physics Letters*, 793 (2022) 139459.